

Synthesis, Characterization, and Morphology of Model Graft Copolymers with Trifunctional Branch Points

Samuel P. Gido,* Chin Lee, and Darrin J. Pochan

Department of Polymer Science and Engineering, University of Massachusetts Amherst, Amherst, Massachusetts 01003

Stergios Pispas† and Jimmy W. Mays*

Department of Chemistry, University of Alabama at Birmingham, Birmingham, Alabama 35294

Nikos Hadjichristidis

Department of Chemistry, University of Athens, Panepistimiopolis Zografou 15771, Athens, Greece, and Institute of Electronic Structure and Laser, 711 10 Heraklion, Crete, Greece

Received May 16, 1996; Revised Manuscript Received August 2, 1996[®]

ABSTRACT: Well-defined graft copolymers with polyisoprene backbones and polystyrene branches, having trifunctional branch points, of the type S_2IS_2 (H-shaped) and (SI)I(SI) (π -shaped) were synthesized by anionic polymerization high-vacuum techniques. The synthetic strategy involves the preparation of the outer parts of the molecules, carrying one reactive Si–Cl bond, followed by coupling with difunctional living poly(isoprenyllithium) chains. In this way, the number and placement of the branches can be precisely controlled. Molecular characterization of the fractionated samples by size exclusion chromatography with UV and RI detection, membrane osmometry, low-angle laser light scattering, and ¹H-NMR spectroscopy confirmed that the materials exhibit narrow molecular weight distributions and low compositional heterogeneity. The strongly microphase-separated morphologies of these two samples were characterized using TEM and SAXS. The π architecture with a PS volume fraction of 0.21 was found to form body-centered cubic spheres, while the H architecture with a PI volume fraction of 0.64 was found to form a lamellar morphology. The observed morphology for these architectures was rationalized by formally dividing the π and H architectures into component simple (single) graft block copolymers which were mapped onto Milner's morphology diagram for simple graft copolymers.

1. Introduction

Graft copolymers are a class of nonlinear block copolymers, which due to their biphasic nature and architecture show interesting solution, mechanical, and morphological properties which allow their use as thermoplastic elastomers, compatibilizers of polymer blends and viscosity modifiers.¹ Anionic polymerization techniques have been widely used for the preparation of well-defined (with respect to molecular weight of the branches and the backbone) graft copolymers.^{2–13} However, apart from a few exceptions,^{10–13} the number of grafts and their position on the backbone have been controlled to a lesser extent.

In the present paper, we report on the synthesis, molecular characterization, and morphology of model graft copolymers with polyisoprene backbones and polystyrene branches. These molecules have two trifunctional branch points at the end of the backbone (S_2IS_2 : H-shaped copolymer) or equally spaced along the backbone ((SI)I(SI): π -shaped or double graft copolymer). The architectures of these novel materials are shown in Figure 1a,b. A similar block copolymer "super-H" architecture has been recently synthesized and characterized.^{12,27}

We have recently completed a morphological study of simple graft block copolymers of polystyrene (PS) and polyisoprene (PI).^{14,15} The molecular architecture of

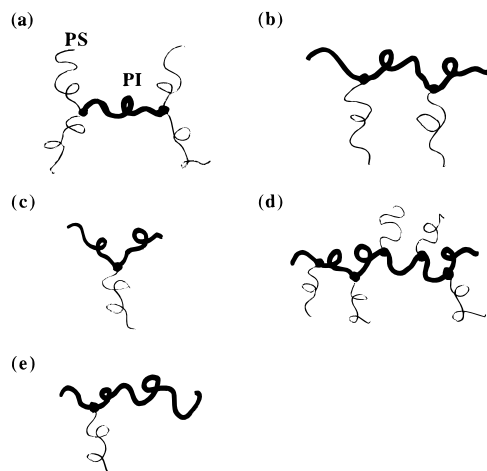


Figure 1. Graft block copolymer molecular architectures: (a) S_2IS_2 or H-shaped architecture, (b) (SI)I(SI) or π -shaped architecture, (c) I_2S simple graft architecture, (d) complex graft architecture, and (e) off-center simple graft architecture.

these simple graft copolymers is shown in Figure 1c: A single PS block is grafted midway along a PI backbone. In the notation of Olvera de la Cruz and Sanchez,¹⁶ this corresponds to a simple graft structure in which $\tau = 0.5$, where τ is the fractional distance along the PI backbone at which the PS graft occurs. For PS component volume fractions from 0.08 to 0.91, the ranges in which various morphologies were observed were shifted to higher PS volume fractions, in general agreement with the theoretical predictions of Milner¹⁷ for graft chain architectures. Milner's predicted morphology diagram for simple grafts is reproduced in Figure 2. Only one of our simple

* To whom correspondence should be addressed.

† Present address: Department of Chemistry, University of Athens, Panepistimiopolis Zografou 15771, Athens, Greece.

© Abstract published in *Advance ACS Abstracts*, September 15, 1996.

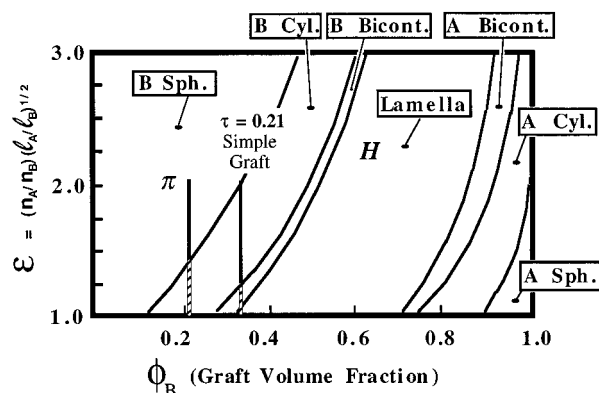


Figure 2. Theoretical morphology diagram calculated by S. T. Milner for two-component miktoarm star block copolymers. This diagram includes the symmetric simple graft behavior for ϵ close to 2. The symbol H indicates the mapping of the H architecture onto the diagram by formally dividing it into component simple grafts. The bold segments of the vertical lines at graft volume fractions of 0.21 and 0.33 represent the allowable range of ϵ for the partitioning of the π architecture and for an off-center simple graft material, respectively.

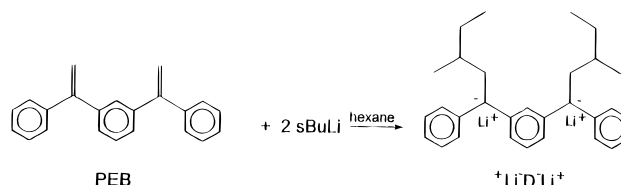
graft samples deviated from the predictions of this diagram; the sample at 0.81 PS graft volume fraction formed a new, randomly ordered, wormlike micelle structure,¹⁵ which was demonstrated to be an equilibrium structure by careful annealing experiments.¹⁴

Our goal is to use a knowledge of simple graft morphological behavior as a building block to an understanding of the morphological behavior of more complex multigraft molecular architectures. One might envision that to a first approximation a complex molecular architecture, such as that shown in Figure 1d, may be decomposed into component simple grafts and that general rules may be discovered that govern how the composition and architecture of the component simple grafts, and the way in which they are linked together, influence the morphology formed by the overall molecule. Such a process could in general involve component simple grafts in which the graft is not symmetrically located along the backbone, as shown in Figure 1e. We are also studying the behavior of such off-center simple grafts as part of the overall research effort.¹⁸ In this paper, we discuss the synthesis, molecular characterization, and morphological characterization results on two of the simplest possible multigraft block copolymer architectures, the π and H . In the π architecture of this study, two PS blocks of equal length are grafted at positions $\tau = 0.35$ and 0.65 along a PI backbone. The π architecture can be thought of, approximately, as two simple graft copolymers joined together at the ends of the PI backbones. The H architecture can be thought of as two simple graft copolymers where two PS backbones share a common centrally grafted PI block. In this initial study, one π and one H graft copolymer morphology was synthesized and characterized. The π architecture had a PS volume fraction of 21%, and the H architecture had a PS volume fraction of 36%.

2. Experimental Section

Purification and Polymerization Procedures. All reagents used (solvents, monomers, and linking and terminating agents) were purified using standard high-vacuum anionic polymerization techniques.¹⁹ Polymerizations and linking reactions were carried out in all-glass n -BuLi-washed and benzene-rinsed reactors. The grafts and the backbones were synthesized in separate reactors and linked together in the

Scheme 1

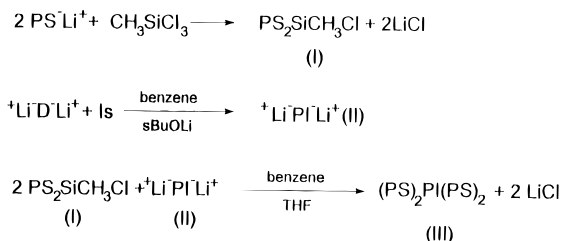


appropriate fashion, in order to obtain the desired architecture, using chlorosilane chemistry.^{10–13} Benzene was the solvent in all cases and s -BuLi, purified by sublimation under high vacuum, was the initiator for the synthesis of the arms (outer parts) of the molecules. A lithium-based difunctional initiator was used for the preparation of the connecting part of the backbone between the branching points (see below). After the completion of each synthetic step, samples were withdrawn from the main reactors, by heat sealing the appropriate constrictions, in order to characterize the intermediate products. The final linking reactions, between the difunctional connectors and the functional outer parts, were carried out in the presence of a small amount of THF. The graft copolymers were separated from the undesired byproducts by fractionation in toluene/methanol mixture and dried under vacuum.

Synthesis of the Difunctional Initiator and the Connectors. For the synthesis of the connecting part of the backbone, in both cases the difunctional initiator (1,3-phenylene)bis(3-methyl-1-phenylpentylidene)dilithium (DLi) was prepared by the reaction of 1,3-bis(1-phenylethenyl)benzene (PEB) and s -BuLi in hexane solution²⁰ in an all-glass reactor, purged in the usual manner, under high-vacuum conditions (Scheme 1).

A slight excess of s -BuLi ($\sim 10\%$) was used in order to ensure difunctionality of the final product.²¹ PEB was prepared using literature procedures.²² It was purified on the vacuum line by drying over CaH_2 and exposure to n -BuLi before the final sublimation, diluted with hexane, and subsequently divided into ampoules equipped with break seals. The difunctional initiator is insoluble in hexane. After completion of the reaction, the precipitated product was separated from the supernatant solution by filtration and washed repeatedly from the remaining unreacted s -BuLi by distillation of hexane into the reaction flask. Finally, the solvent containing the unreacted materials was separated from the main reactor by heat sealing. The reactor was then attached to the vacuum line through a break seal, and purified benzene was distilled into the apparatus, producing a solution of $\sim 2.5 \times 10^{-5}$ mol/mL of the difunctional initiator, which was subdivided into calibrated ampoules for further use. An aliquot of this solution was hydrolyzed and divided into two portions. The first one was titrated with aqueous hydrochloric acid in order to determine the total Li concentration. From the second aliquot the solid product of the reaction was isolated by evaporation of the solvent and analyzed by ^1H -NMR spectroscopy in order to check the purity of the initiator. Test polymerizations of isoprene were run in benzene in the presence of s -BuOLi (prepared by reaction of s -BuOH and s -BuLi) in order to check the difunctionality of the initiator by aid of the resulting molecular weight, the known amount of the monomer used, and the total concentration of Li determined by titration.²³ Very close agreement between the calculated stoichiometric molecular weights, assuming perfect difunctionality, and the experimentally determined molecular weights was observed, confirming the NMR result that the organolithium compound isolated was the desired product. In the same manner, the connecting polyisoprene chains for the graft copolymers were synthesized, always taking precautions to minimize contact of the initiator with impurities, coming mainly from the glass surface of the reactors, using purged glassware. The molecular weight distributions of the resulting polyisoprenes, determined by SEC, were always monomodal, with tails at the high elution volume region of the chromatogram and polydispersities around 1.2 (depending also on the molecular weight of the polymer) due to the slow initiation reaction.^{20,23} ^1H -NMR analysis revealed that the polyisoprenes prepared in this way

Scheme 2



had low vinyl content ($\sim 7\%$), identical to specimens prepared by *s*-BuLi, ensuring uniformity in the microstructure of the backbone and low T_g for the polyisoprene phase.

Molecular Characterization. The molecular weight distributions and purity of the final graft copolymers and the intermediate products were checked by size exclusion chromatography in THF at 35 °C (Waters 510 pump, Waters Model 410 differential refractometer, LDC/Milton Roy variable-wavelength UV detector in series with three Phenomenex linear columns). Number-average molecular weights were measured with a Wescan Model 231 membrane osmometer in toluene at 37 °C. Weight-average molecular weights of the grafts were measured with a Chromatix KMX-6 low-angle laser light scattering photometer operating at 633 nm, in THF at 25 °C. The specific refractive index increments, dn/dc , required for the light scattering measurements were determined with an Otsuka DRM-1020 differential refractometer at the same wavelength, temperature, and solvent. Composition of the copolymers was determined by SEC-UV at 260 nm, after calibration with several concentrations of polystyrene standards, and ^1H -NMR spectroscopy (Bruker 400 MHz).

Morphological Characterization. Solid films approximately 2 mm thick of the π and H graft block copolymers were slowly cast from 5 wt % polymer solutions in toluene, a nonpreferential solvent. Casting was performed at room temperature, and the evaporation of solvent was controlled to form a solid film after 10–14 days. The films were given several more days at room temperature and atmospheric pressure and an additional several days under high vacuum at room temperature in order to remove residual solvent. The samples were then annealed for 1 week under high vacuum at 120 °C in order to further promote the approach to an equilibrium structure.

After annealing, samples for electron microscopy were microtomed in a Reichert-Jung cryoultramicrotome. Sections approximately 300–800 Å thick were cut with a Diatome diamond knife at a sample temperature of -110 °C and a knife temperature of -90 °C. The sections were stained in OsO_4 vapors for 4 h. Transmission electron microscopy (TEM) was performed on a JEOL 100CX operated at 100 kV accelerating voltage. SAXS experiments were performed on annealed films using a Rigaku-Denki camera with Cu $K\alpha$ sealed-tube X-ray radiation and pinhole collimation. Patterns were recorded photographically with Kodak direct-exposure X-ray film (DEF-5). SAXS patterns were digitized with an Agfa Arcus II flat bed scanner and analyzed with custom-written software.

3. Results

Synthesis. The synthetic strategy used for the preparation of the S_2IS_2 copolymer is shown in Scheme 2 and is analogous to the one used by Roovers and Toporowski²⁴ for the synthesis of the H-shaped polystyrene homopolymers. The corresponding SEC chromatograms are given in Figure 3.

Living poly(styryllithium) (Figure 3a) was reacted with CH_3SiCl_3 in a 2.1:3 Li/Cl ratio. Due to steric hindrances, only coupled material was formed with no detectable amount of three arm star material (Figure 3b). After the formation of the polyisoprene connector (Figure 3c), the difunctional living polymer was reacted with the polystyrene dimer, having a reactive Cl at the middle of the chain, in a 1:2.2 ratio. A small excess of

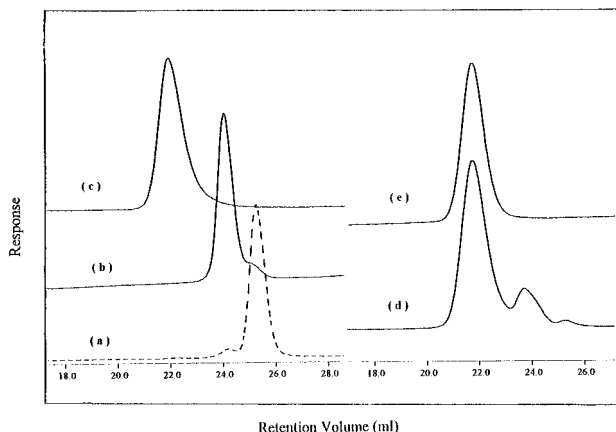
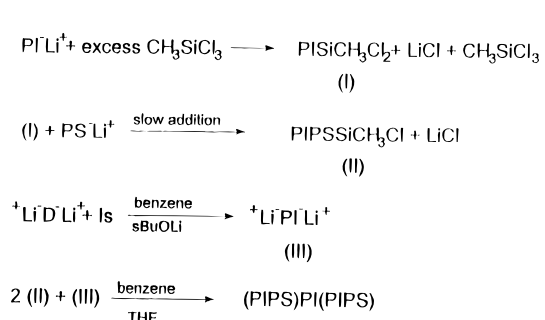


Figure 3. SEC chromatograms from the synthesis of the S_2IS_2 (H-shaped) copolymer: (a) PS arm (the peak at high elution volume is due to deactivation of the sample solution under nonanaerobic conditions); (b) product of the reaction of PS arm with CH_3SiCl_3 (Li/Cl = 2.1/3); (c) difunctional PI connector ($M_w/M_n = 1.19$); (d) crude product of the coupling reaction (first peak, graft copolymer; second peak, excess of coupled PS arms, third peak, excess PS arm from step 3b), (e) fractionated S_2IS_2 copolymer.

Scheme 3



arms was used in order to ensure complete end-capping of the connector. A small amount of THF ($\sim 0.3\%$ v/v) accelerates the coupling reaction by decreasing the degree of association of the poly(isoprenyllithium) ends. The resulting H-copolymer is free of high molecular weight byproducts, as can be seen from the corresponding SEC chromatogram of the unfractionated material (Figure 3d), indicating that this approach is better than the one used for the preparation of the super-H copolymers.¹² Fractionation resulted in a sample free of byproducts which exhibited a narrow molecular weight distribution.

The reaction sequence for the synthesis of the π -shaped copolymer is shown in Scheme 3, and the corresponding SEC chromatograms are presented in Figure 4. In this case, the preparation starts from the synthesis of the outer parts of the polyisoprene backbone. Living poly(isoprenyllithium) with molecular weight about one-third of the backbone is end-capped with CH_3SiCl_3 (Figure 4b,c). A large excess of the linking agent ensures that only one Cl reacts with the living polymer. However, due to the lower steric hindrance of the poly(isoprenyllithium) chain end (as compared to PS), some coupled material ($\sim 2.5\%$) can be seen in the chromatogram of the end-capped product (Figure 4c). The excess CH_3SiCl_3 was removed on the vacuum line over several days. Living poly(styryllithium) (Figure 4a), the branch, was slowly added to the pure difunctional macromolecular agent until complete substitution of the second Cl connected to the Si. Since polycondensation products can be formed in the

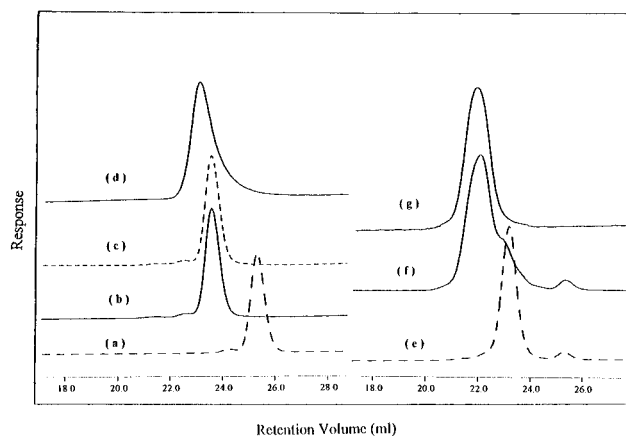


Figure 4. SEC chromatograms from the synthesis of the (SI)I(SI) or π -shaped copolymer: (a) PS branch, (b) PI arm, (c) PI arm after the capping reaction with CH_3SiCl_3 ; (d) PI connector ($M_w/M_n = 1.26$), (e) product of the titration of 4c with 4a (first peak, functional diblock arm with one reactive Cl located at the junction point; second peak, excess of PS branch); (f) crude product of the coupling reaction between 4d and 4e; (g) fractionated (SI)I(SI) copolymer.

Table 1. Molecular Characteristics of Model Graft Copolymers

sample	$M_w^a \times 10^{-4}$	$A_2^a \times 10^{-4}$	$M_n^b \times 10^{-4}$	$A_2^b \times 10^{-4}$	M_w/M_n	% PS ^d	$M_n^b \times 10^{-4}$			
							wt	PS arm	PI arm	PI con
S_2IS_2	17.4	8.09	17.1	7.66	1.08	42	2.03			10.2
(SI)-I-(SI)	14.7	9.47	13.3	8.99	1.09	24	1.91	3.72	3.33	

^a By LALLS in THF at 25 °C. ^b By membrane osmometry in toluene at 37 °C. ^c By SEC in THF at 35 °C. ^d By SEC-UV in THF (note: by $^1\text{H-NMR}$, S_2IS_2 : 43% wt PS, (SI)-I-(SI): 24% wt PS).

next step (which involves the coupling of the centrally functional diblock with the difunctional connector) if two chlorines are present on the macromolecular coupling agent, a small excess of poly(styryllithium) was added beyond the end point of the titration, resulting in a slightly yellow solution (Figure 4e). The color remained stable until this solution was used for the final reaction (about 1 week), indicating that the third Cl is not readily substituted by PSLi. The peak corresponding to the PS branch is evident in the SEC chromatogram of the final crude product (Figure 4f) of the coupling reaction between the connector (Figure 4d) and the diblock arms, showing that even in the presence of THF the reaction of PSLi with the third Cl is not favored in contrast to the case of PILi. Fractionation of the crude product resulted in the pure double-graft material (Figure 4g).

Molecular Characterization. The molecular characteristics of the purified model graft copolymers are shown in Table 1. There is good agreement between the weight- and the number-average molecular weights of the copolymers determined by absolute methods, supporting the result from SEC with RI and UV detection and confirming that these materials have narrow molecular weight distributions and low compositional heterogeneity. The number-average molecular weights of the copolymers are close to the sums of the molecular weights of the branches and the backbone. The chemical composition determined by spectroscopic methods and from the number-average molecular weights of the different parts of the molecules agree closely. Finally, the experimentally determined specific refractive indices for the graft samples (0.153 for the H copolymer and 0.143 for the π -shaped copolymer) are nearly equal to the ones calculated from the weight

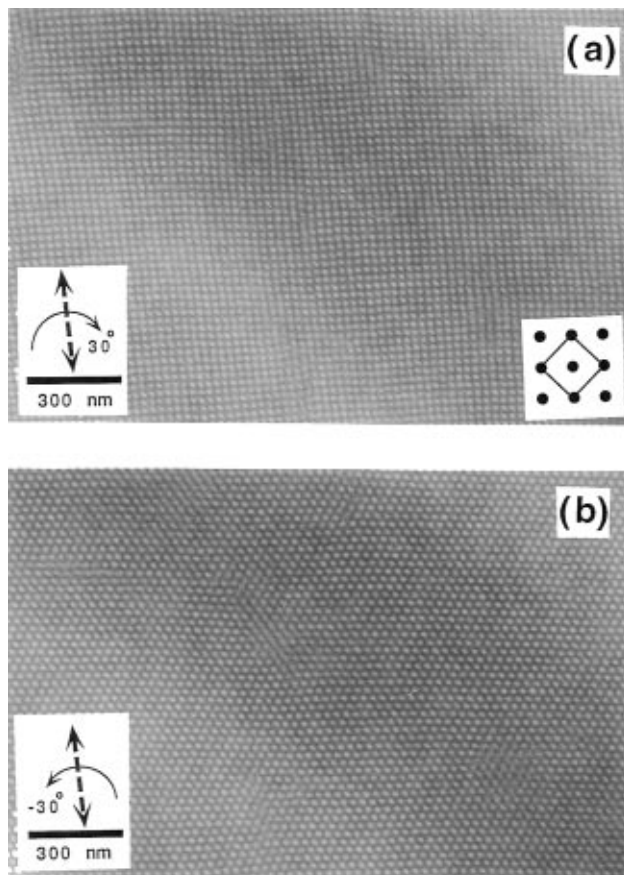


Figure 5. Tilt series of TEM images of the π material: (a) square pattern produced by projection along the [100] direction (edge) of the bcc unit cell; (b) hexagonal pattern produced by projection along the [111] direction (body diagonal) of the bcc unit cell.

fractions of each component and the dn/dc values cited in the literature for the corresponding homopolymers¹² ($\{dn/dc\}_{\text{cop}} = x\{dn/dc\}_{\text{PS}} + (1-x)\{dn/dc\}_{\text{PI}}$, where x is the weight fraction of PS). The above results conclusively establish that the samples actually possess the predicted architectures and can be characterized as model materials due to their molecular weight and compositional uniformity along with their well-defined structure and molecular characteristics.

Morphology. The results of the morphological characterization indicate that the π architecture with 0.21 volume fraction for the two PS grafts (combined) yields a body-centered cubic (bcc) packing of spherical PS microdomains in a PI matrix. The results of the morphological characterization indicate that the H architecture, with a combined volume fraction of 0.36 for the four PS blocks, yields a lamellar morphology. Figure 5 shows a TEM tilt series of the π material in which a relative tilt of approximately 60° changes the image from a square pattern of projected spheres (Figure 5a) to a hexagonal pattern (Figure 5b). The axis around which this tilt occurs, indicated by a double-headed dashed arrow, is along a face diagonal of the bcc unit cell. Geometrically, a tilt of 55° about this axis is required to go between the square projection along the [100] direction (unit cell edge) and the hexagonal projection along the [111] direction (body diagonal). The relative tilt in this experimental series is close enough to the calculated value to provide strong evidence for the bcc structure. Note that because the structure is bcc rather than simple cubic (sc), the smallest square arrangement of spheres in Figure 5a does not represent

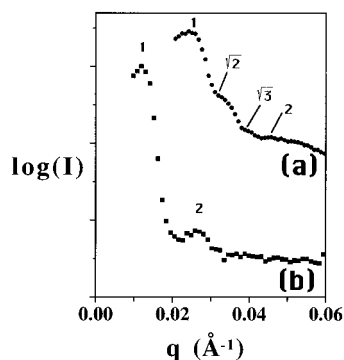


Figure 6. SAXS patterns with scattering vector ratios indicated for (a) the π material and (b) the H material.



Figure 7. TEM micrograph of the lamellar morphology produced by the H material.

a projection of the unit cell. As indicated by the inset, the bcc unit cell is actually rotated by 45° and contains a sphere in the center. Thus the indicated tilt axis is seen to truly be around a face diagonal of the cubic cell. The SAXS pattern in Figure 6a shows four reflections with ratios q_n/q^* , of the n th reflection scattering vector to the first reflection scattering vector, of 1, $\sqrt{2}$, $\sqrt{3}$, and 2. The two higher angle reflections are difficult to see in the figure but are clearly visible on the original photographic negative. This series of q_n/q^* is characteristic of cubic structures and is consistent with both bcc and sc structures. Figure 7 shows a TEM micrograph of the lamellar morphology produced by the H graft copolymer sample. The SAXS data in Figure 6b show two peaks with q_n/q^* ratios of 1 and 2. This is characteristic of the one-dimensional lattice of the lamellar morphology.

4. Discussion

We hope to devise a method by which Milner's morphology diagram (Figure 2) can be adapted to shed



Figure 8. Formal division of the π and H molecular architectures into component simple graft block copolymers for the purpose of mapping the morphological behavior onto the simple graft morphology diagram.

light on the morphological behavior of more complex graft copolymers such as the π and H architectures. This morphology diagram incorporates the strong segregation behavior of the general class of A_nB_m stars, which includes as special cases diblocks ($n = m = 1$) and symmetric simple graft copolymers ($n = 2, m = 1$).

In order to apply the A_nB_m morphology diagram to graft architectures, we must find appropriate rules of thumb for decomposing the complex graft architecture into its component simple grafts. As shown in Figure 8, one can postulate dividing either the π or the H graft architecture into two component simple grafts by cutting the connecting block in the middle. Other schemes might also be postulated. In the H architecture, dividing the molecule in the center of the bridging PI block leads to symmetric simple grafts ($\tau = 1/2$) with the PI block as the graft block, and a PI volume fraction of 0.64 for each of these component simple grafts, the same as the overall molecule. In the π architecture, if the central PI block is imagined to be cut in half, then the π architecture is decomposed into two asymmetric simple grafts ($\tau \approx 1/3$), with PS (graft block) volume fractions of 0.21, the same as the overall molecule.

In Milner's morphology diagram, the calculation of the ϵ parameter assumes that all blocks of the same type are of the same length (molecular weight). This assumption does not hold true for asymmetric simple grafts such as those into which the π architecture is decomposed by cutting the connecting PI block in the middle. The lateral crowding and additional chain stretching associated with the two chains on one side of the interface in a simple graft architecture should be partially alleviated in an asymmetric graft architecture. It is desirable to generalize the ϵ parameter in order to account for the different effect on chain conformation of different graft locations, τ , and to then apply that generalized ϵ to map asymmetric graft behavior onto the same morphology diagram as in Figure 2. Such an approach may or may not be theoretically justified. It may turn out that one cannot keep the same phase boundaries as in Figure 2 and simply modify ϵ . The boundaries may be different with asymmetric simple grafts; just how different these boundaries would be is unknown at this time.²⁵ With these caveats in mind, we now proceed to try and map our experimental data for π and H architectures onto the morphology diagram in the hope that the unknown shift in the morphology boundaries will be slight.

We postulate the following type of relationship: $\epsilon = f(\tau)(I_a/I_b)^{1/2}$. When $\tau = 0$ or 1, then ϵ should represent diblock behavior: $\epsilon = (I_a/I_b)^{1/2}$. When $\tau = 0.5$, then ϵ should represent symmetric simple graft behavior: $\epsilon = 2(I_a/I_b)^{1/2}$. Between $\tau = 0$ and 0.5, the value of ϵ must vary continuously between $(I_a/I_b)^{1/2}$ and $2(I_a/I_b)^{1/2}$. Since the choice of which end of the backbone to designate as position 0 and which to designate as 1 is arbitrary, the same behavior of ϵ vs τ must be obtained as τ is varied from 1.0 to 0.5. The function of ϵ vs τ must be

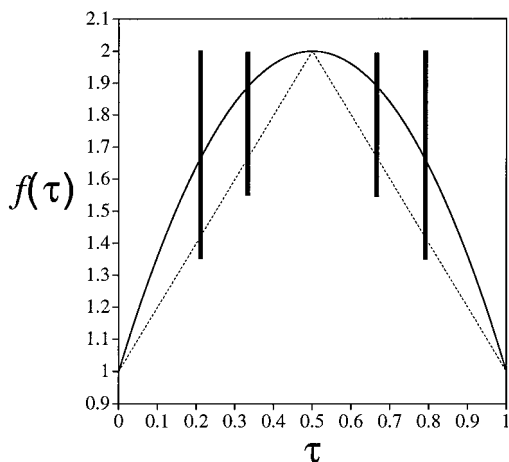


Figure 9. Possible $f(\tau)$ relationships. Bold vertical bars at $\tau = 0.21, 0.35, 0.65$, and 0.79 represent allowable ranges of $f(\tau)$ values. The two curves shown are a second-order polynomial and a linear relationship.

continuous at $\tau = 0.5$ and possess a horizontal tangent at this point: $\partial\epsilon/\partial\tau = 0$ at $\tau = 0.5$.

Since the partitioning of the H graft architecture gives two identical symmetric simple grafts, it is straightforward to calculate ϵ to be 2.25. This value is different from the value (1.78) found for the PS-PI simple graft architectures in our previous publications.^{14,15} This is because in the partitioning of the H architecture PI, rather than PS, ends up comprising the grafted block. Thus the factor $(I_g/I_b)^{1/2}$ is the reciprocal of that used in our previous work. The partitioning of the H graft is plotted on the theoretical morphology diagram in Figure 2. With this partitioning scheme, the H graft is mapped into the middle of the lamellar region of the diagram, in agreement with the experimental observation of a lamellar morphology. If the π architecture is partitioned by cutting the connecting block in half, then the observed morphology should fall on a vertical line on the morphology diagram at a graft block volume fraction of 0.21. The position along this line depends on the unknown ϵ vs τ relationship, since $\tau = 0.35$. However, because we have a spherical morphology, we know that ϵ must be greater than about 1.4, to place us on the part of the vertical line in the spherical region of the diagram.

We can further constrain the ϵ vs τ relationship at $\tau = 0.21$, with results from another ongoing study of asymmetric simple graft block copolymers.¹⁸ In this study, one sample has a PI backbone (65 900 g/mol) to which is grafted a single PS chain (31 600 g/mol) at position $\tau = 0.21$. This material with a PS graft volume fraction of 0.33 was found to have a cylindrical morphology. A vertical line on the morphology diagram at volume fraction 0.33 represents this structure. In order to be in the cylindrical region of the morphology diagram, ϵ must be greater than 1.2. With this information, we can place an additional lower bound on the value of ϵ at $\tau = 0.21$. And, since $(I_{PI}/I_{PS})^{1/2}$ is 0.89, we can place limits on $f(\tau)$: $1.2 < \epsilon$, and thus $1.35 < f(\tau)$ at $\tau = 0.21$; $1.4 < \epsilon$, and thus $1.57 < f(\tau)$ at $\tau = 0.35$.

Figure 9 shows graphs of several possible $f(\tau)$ functions. Bold vertical bars at $\tau = 0.21, 0.35, 0.65$, and 0.79 represent the allowable range as established by lower bounds at these values of τ . A linear relationship and a second-order polynomial are shown which intersect the allowable range. Half of a period of a sine wave produces a curve which is very close to the second-order

polynomial. The linear relationship does not, however, have the required continuity and horizontal tangent at $\tau = 1/2$. Obviously, to experimentally establish the f vs τ function will require much more data. However, it is clear that for τ close to zero that the system behaves like a diblock. As τ increases, it appears that the behavior rapidly takes on a simple graft character in which the lateral crowding and additional chain stretching of the two arms on one side of the interface can alter the morphology from that observed for a simple linear diblock. This shift in the morphological behavior is maximized for the symmetric simple graft ($\tau = 0.5$). The behavior of the two PI chains, when of different lengths, should be similar to a bimodal end-grafted polymer brush, which has been investigated theoretically.²⁶

5. Conclusions

This paper encompasses a broad range of work involving well-defined π - and H-shaped block copolymer multigraft architectures. The anionic synthetic strategies for both these molecules involved separate synthesis of PI and PS blocks, followed by controlled end linkage, with chlorosilane chemistry, to form the desired architectures. The molecules so synthesized were characterized using size exclusion chromatography, membrane osmometry, low-angle laser light scattering, and ¹H-NMR. This characterization work confirmed the desired molecular architectures and narrow molecular weight distributions.

The strongly microphase-separated morphologies of these two samples were characterized using TEM and SAXS. The π architecture with a PS volume fraction of 0.21 was found to form body-centered cubic spheres, while the H architecture with a PI volume fraction of 0.64 was found to form a lamellar morphology. An attempt was made to rationalize the observed morphology for these architectures by formally dividing the π and H architectures into component simple (single) graft block copolymers. These components were mapped onto Milner's morphology diagram for simple grafts. In order to map the asymmetric simple graft components of the π architecture onto the morphology diagram, a general form of the relationship between Milner's molecular asymmetry parameter, ϵ , and the fractional location of the graft along the backbone, τ , was postulated. Although we do not yet possess enough experimental data to fully determine the relationship between ϵ and τ , the results of this paper allow us to put some bounds on this relationship. The result is a mapping of the π and H architectures onto the simple graft morphology diagram which is consistent with the experimentally observed morphologies. Experimental work with a more complete set of π and H samples has been initiated.²⁸

Acknowledgment. S.P.G., D.J.P., J.W.M., and S.P. would like to acknowledge funding from the Army Research Office under Contract DAAH04-94-G-0245. Additionally, S.P.G. acknowledges an Army Young Investigator Award (DAAH04-95-1-0305). We acknowledge the use of TEM instrumentation in the W. M. Keck Polymer Morphology Laboratory at the University of Massachusetts Amherst, ARO instrumentation funding (DAAH04-95-1-0005), and Central Facility Support from the Materials Research Science and Engineering Center (MRSEC) at the University of Massachusetts Amherst.

References and Notes

- (1) Dreyfuss, P.; Quirk, R. P. In *Encyclopedia of Polymer Science and Engineering*; Mark, H. F., Bikales, N. M., Overberger,

- C. G., Menges, G., Kroschwitz, J. I., Eds.; Wiley-Interscience: New York, 1987; Vol. 7; pp 551-579.
- (2) Price, C.; Woods, D. *Polymer* **1973**, *14*, 82.
 - (3) Candau, F.; Afchar-Taromi, F.; Rempp, P. *Polymer* **1977**, *18*, 1253.
 - (4) Selb, J.; Gallot, Y. *Polymer* **1979**, *20*, 1273.
 - (5) Selb, J.; Gallot, Y. *Polymer* **1979**, *20*, 1259.
 - (6) Rahlves, D.; Roovers, J. E. L.; Bywater, S. *Macromolecules* **1977**, *10*, 604.
 - (7) Hadjichristidis, N.; Roovers, J. E. L. *J. Polym. Sci., Polym. Phys. Ed.* **1978**, *16*, 851.
 - (8) Se, K.; Watanabe, O. *Makromol. Chem., Macromol. Symp.* **1989**, *25*, 249.
 - (9) Bayer, U.; Stadler, R. *Macromol. Chem. Phys.* **1994**, *195*, 2709.
 - (10) Mays, J. W. *Polym. Bull.* **1990**, *23*, 249.
 - (11) Iatrou, H.; Siakali-Kioulafa, E.; Hadjichristidis, N.; Roovers, J.; Mays, J. W. *J. Polym. Sci., Polym. Phys. Ed.* **1995**, *33*, 1925.
 - (12) Iatrou, H.; Avgeropoulos, A.; Hadjichristidis, N. *Macromolecules* **1994**, *27*, 6232.
 - (13) Iatrou, H.; Hadjichristidis, N. *Macromolecules* **1993**, *26*, 2479.
 - (14) Pochan, D. J.; Gido, S. P.; Pispas, S.; Mays, J. W. *Macromolecules* **1996**, *29*, 5099.
 - (15) Pochan, D. J.; Gido, S. P.; Pispas, S.; Mays, J. W.; Ryan, A. J.; Fairclough, J. P. A.; Hamley, I. W.; Terrill, N. J. *Macromolecules* **1996**, *29*, 5091.
 - (16) Olvera de la Cruz, M.; Sanchez, I. C. *Macromolecules* **1986**, *19*, 2501.
 - (17) Milner, S. T. *Macromolecules* **1994**, *27*, 2333.
 - (18) Gido, S. P.; Pochan, D. J.; Lee, C.; Pispas, S.; Mays, J. W., to be published.
 - (19) Morton, M.; Fetters, L. J. *Rubber Chem. Technol.* **1975**, *48*, 359.
 - (20) Tung, L. H.; Lo, G. Y.-S. *Macromolecules* **1994**, *27*, 2219.
 - (21) Guyot, P.; Favier, J. C.; Uytterhoven, M.; Fontanille, M.; Sigwalt, P. *Polymer* **1981**, *22*, 1724.
 - (22) Ignatz-Hoover, F. Ph.D. Thesis, University of Akron, 1989.
 - (23) Quirk, R. P.; Ma, J.-J. *Polym. Int.* **1991**, *24*, 197.
 - (24) Roovers, J.; Toporowski, P. *Macromolecules* **1981**, *14*, 1174.
 - (25) Milner, S. T., personal communication.
 - (26) Milner, S. T.; Witten, T. A.; Cates, M. E. *Macromolecules* **1989**, *22*, 853.
 - (27) Iatrou, H.; Willner, L.; Hadjichristidis, N.; Halperin, A.; Richter D. *Macromolecules* **1996**, *29*, 581.
 - (28) Gido, S. P.; Lee, C.; Mays, J. W.; Poulos, Y.; Hadjichristidis, N., to be published.

MA960715F